LATTICE DESIGN FOR THE LHEC RECIRCULATING LINAC*

Yi-Peng Sun and Chris Adolphsen, SLAC, Menlo Park, USA
Anders Lund Eide and Frank Zimmermann, CERN, Geneva, Switzerland

Abstract

In this paper, we present a lattice design for the Large Hadron Electron Collider (LHeC) recirculating linac. The recirculating linac consists of one roughly 3-km long linac hosting superconducting RF (SRF) accelerating cavities, two arcs and one transfer line for the recirculation. In two passes through a pulsed SRF linac the electron beam can get a maximum energy of 140 GeV. Alternatively, in the Energy Recovery Linac (ERL) option the beam passes through a CW linac four times (two passes for acceleration and two for deceleration) for a maximum energy of 60 GeV [1].

INTRODUCTION

The Large Hadron Collider (LHC) at CERN started commissioning recently and already achieved a collision energy of 7 TeV. The LHC experiments will provide data at sufficiently high energies, to answer questions related to the Standard Model of Particle Physics (SM). A different machine type, like the LHeC, might be needed to study in detail the character of a phenomenon found at the LHC. A proton-electron collider at TeV-scale center of mass energy based on the LHC was first proposed by F. Close in 1990 [2], to take the place of HERA (Hadron Elektron Ringanlage) at DESY. Two different accelerator types, a storage ring and a linear accelerator, are considered for the LHeC. A storage ring requires less R&D than a linac at the proposed energy. Also it can use the accelerating cavities for many turns to accelerate each particle, which reduces both the construction and operational costs. On the other hand, the installation of a lepton ring in the present LHC tunnel is challenging, and a dedicated separate linac provides the possibility of going to higher energies, lower emittance and high electron polarization. Studies show that for a machine with beam energy between 60 GeV and 140 GeV, one recirculation (two passes through the SRF linac) corresponds to the cost optimum [3].

The accelerator chain of the LHeC Recirculating Linac is composed of one linac with SRF cavities, two arcs and one transfer line, as sketched in Figure 1.

*Work supported by the European Community-Research Infrastructure Activity under the FP6 "Structuring the European Research Area" programme (CARE, contract number RII3-CT-2003-506395), and under the FP7 "Capacities Specific Programme" (EuCARD, under Grant Agreement no 227579). Work also supported by the DOE under Contract DE-AC02-76SF00515.

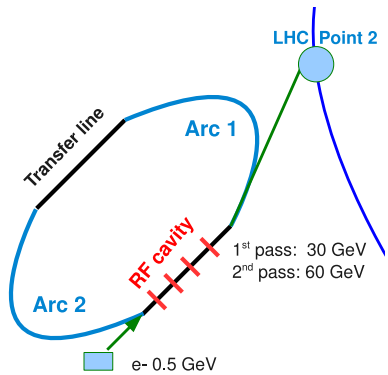

Figure 1: Sketch of the LHeC Recirculating Linac (not to scale).

SRF LINAC

Parameters

The overall parameters for the LHeC Recirculating Linac are listed in Table 1. The 60-GeV ERL option will run with continuous wave mode and thus have a lower SRF accelerating gradient 13 MV/m. All three options have the same cell length of 24 m and SRF cavity fill factor of 0.6 (with spare cells), which is the same as the XFEL design at DESY [4].

Table 1: LHeC Recirculating Linac parameters.

LHeC-RL	Lumi	Baseline	Energy
Final energy [GeV]	60	100	140
Cell length [m]	24	24	24
Cavity fill factor	0.6	0.6	0.6
Linac length [m]	3360	3360	3360
Cav. gradient [MV/m]	13	25	32
Operation mode	CW (ERL)	Pulsed	Pulsed

Linac cell

For electrons traveling near the speed of light ($\beta \approx 1$), the quadrupole focusing length scales linearly with the beam energy

$$f = \frac{\beta E c}{egl} \tag{1}$$

where f denotes the quadrupole focal length, β the velocity relative to the speed of light c, E the beam energy, e the electron charge, g the quadrupole field gradient and l the quadrupole length.

With two passes through the linac for 100 GeV (140 GeV) pulsed option (or four passes for the ERL CW option), the electron beam is focused differently in each pass. Qualitative considerations show that for the normal recirculating linac (without energy recovery), the phase advance per cell can be kept constant in the first pass. The injection energy is chosen as 0.5 GeV and the phase advance per cell is 130 degree in the first pass, which gives 0.7 (54) degree per cell at the beginning (end) of the second pass in the 140 GeV machine, as shown in Figure 2 (left).

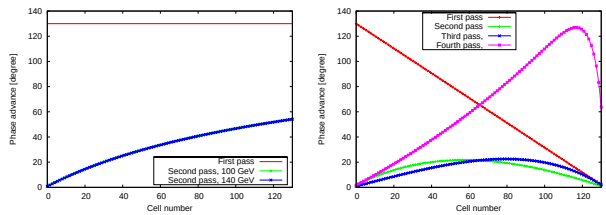

Figure 2: Left: phase advance per cell in both passes through the SRF linac for 100 GeV (140 GeV) pulsed option; Right: phase advance per cell in all the four passes through the SRF linac for the 60 GeV ERL option.

For the ERL we have two additional passes through the SRF linac in which the beam energy is reduced rather than increased. There is no way to keep the phase advance per cell constant in the first pass, as that causes a phase advance of 180 degree only about half way through the fourth pass. Instead the phase advance is chosen to be linearly decreasing from 130 degree to 2 degree in the first pass. This, together with the evolution of the phase advance on the other three passes, is plotted in Figure 2 (right).

There are two cryomodules in each 24 m long SRF linac cell, which accommodate eighteen 5-cell superconducting RF cavities, for an RF frequency of 700 MHz. In Figure 3 the TWISS parameters are plotted, where 18 RF cavities are represented by thin model and distributed between the quadrupoles. The quadrupole gradient increases linearly with energy in the first pass. The maximum and minimum beta functions are 59 m and 4 m, respectively. The drift space (roughly 0.5 m long) can be used to accommodate equipment for beam diagnostics or orbit correction.

Spare cells

Spare 'empty' cells are reserved in the SRF linac, mainly for the hosting of backup RF cavities for energy management in case of klystron failure. The quadrupole strength in the spare cell is set to be the same as the one in the previous cell. An example of the spare cell is shown in Figure 4.

Linac lattice

One spare cell is inserted into the lattice after every 13 normal cells. That means each superperiod contains 13 normal cells plus one spare cell. The whole SRF linac is composed of 10 superperiods. The TWISS parameters of one

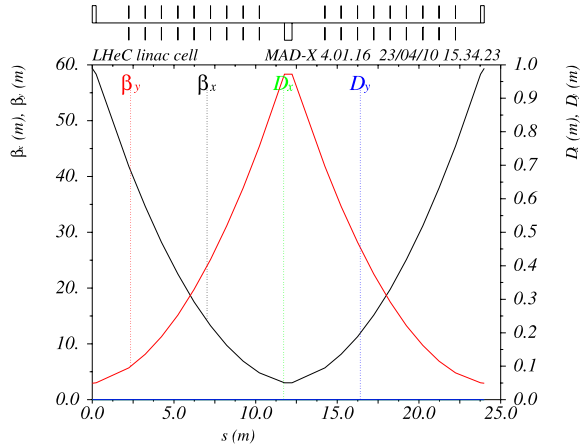

Figure 3: Beta and dispersion functions in one SRF linac cell (first pass), with horizontal and vertical phase advance all equal 130 degree. The quadrupole length is 0.47 m. Optics design is done by using MADX [5].

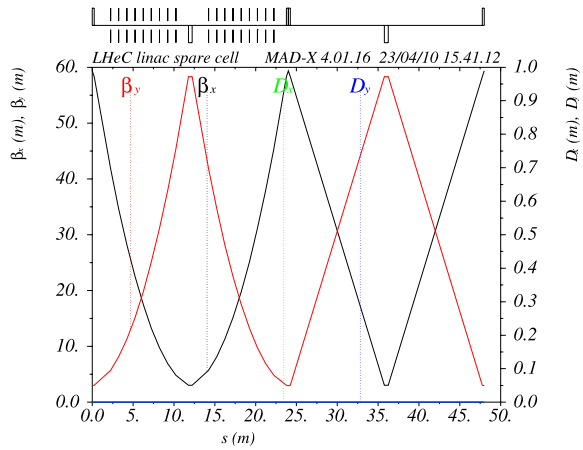

Figure 4: Beta and dispersion functions, for one normal SRF linac cell plus one spare cell.

superperiod are shown in Figure 5 (left), and those of the whole SRF linac in Figure 5 (right).

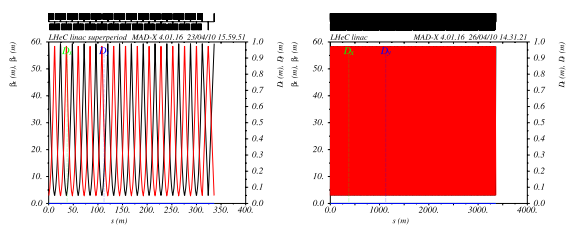

Figure 5: Left: TWISS parameters for one superperiod which is composed of 13 normal cells plus one spare cell; Right: TWISS parameters for the whole SRF linac which has 10 superperiods, and a total length of 3360 m.

All the three scenarios listed in Table 1 can use this same SRF linac for acceleration (plus deceleration for ERL), with a different configuration of klystrons and modulators.

ARC SECTION

Arc cell

The arc of the LHeC Recirculating Linac consists of two identical arc sections, plus one straight transfer line between them. Two correlated effects (energy loss due to synchrotron radiation, and emittance growth from radiation fluctuations) are considered to determine the radius of the arc section. Synchrotron radiation loss is the dominant factor. With $\beta \approx 1$, the electron energy loss per turn is

$$\Delta E = C_\gamma \frac{E^4}{\rho^2} \tag{2}$$

where C_γ denotes Sands radiation constant for electrons [6], E the electron energy and ρ the bending radius.

Considering the highest electron energy in the arc of 70 GeV in the pulsed mode, the radius is chosen to be 1500 m which gives roughly 2% energy loss. The dipole length is 9.8 m and the quadrupole length is 0.47 m. There are 480 arc cells overall. The phase advance per cell is 90 degree in both arc sections and the transfer line. From the calculation of the general transfer matrix with TWISS parameters, and using thin-lens approximation, for the FODO cell we have

$$k = \frac{4\sin(\phi/2)}{l_{cell} l_{quad}} \tag{3}$$

where k denotes the normalized quadrupole strength, ϕ the phase advance of the cell, l_{cell} the cell length and l_{quad} the quadrupole length. Formula (3) is used to estimate the quadrupole strength, then MADX [5] is used to match for the precise value. Figure 6 shows the optics for one arc cell.

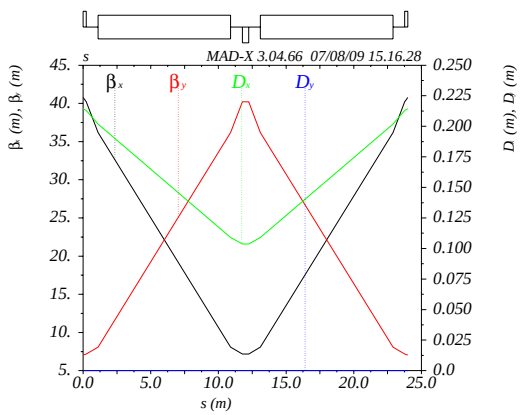

Figure 6: Beta and dispersion functions in one arc cell, with horizontal and vertical phase advance equal to 90 degree.

Dispersion suppressor

To suppress the dispersion generated in the arc dipoles, half-dipole cells (at 50% dipole strength plus one more full cell for 90 degree phase advance) are inserted at the beginning and end of the arc. With four dispersion suppressors, the dispersion and its derivative go to zero at the entrances of the linac and of the transfer line.

SUMMARY

A brief summary of the elements for the three scenarios is given in Table 2. The overall TWISS parameters in the entire machine (with two passes in the SRF linac) are plotted in Figure 7. In the transition regions between arc and SRF linac, several FODO cells are inserted with variable quadrupole strengths to match the TWISS parameters. For the second pass of the pulsed options (or the last three passes in the ERL option), we observe large β-functions in the transition regions where further matching work is needed.

Table 2: LHeC Recirculating Linac elements summary.

LHeC-RL	**Lumi**	**Baseline**	**Energy**
# of RF cavities	2224	2224	2224
# of dipoles	960	960	960
# of quads	1516	1516	1516
Bending radius [m]	1485	1485	1485
Dipole strength [T]	0.073	0.118	0.163
Max quad gradient [T/m]	30	50	78

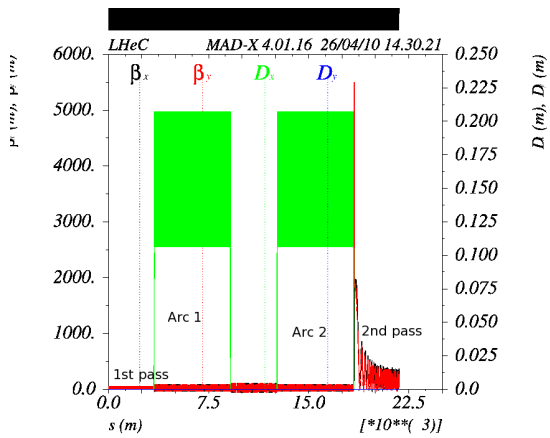

Figure 7: TWISS parameters along the full LHeC Recirculating Linac (two passes through the SRF linac for beam energy of 140 GeV).

We acknowledge helpful discussions with D. Schulte of CERN.

REFERENCES

[1] A. Eiders, Optics Development for the Recirculating Linac of a High-Energy Hadron-Lepton Collider (LHeC) at the LHC, NTNU Project Thesis (2009).

[2] F. Close, Nucl Phys B (Proc Suppl) **21**: 423-429 (1991).

[3] J. Skrabacz, CERN-AB-Note-2008-043 (2008).

[4] M. Altarelli et al., The Technical Design Report of the European XFEL, DESY (2007).

[5] MADX manual, http://mad.web.cern.ch/mad/.

[6] M. Sands, SLAC Report 121 (1970).